Paleometeorology: High resolution Northern Hemisphere wintertime mid-latitude dynamics during the Last Glacial Maximum

M. B. Unterman,[1] T. J. Crowley,[1] K. I. Hodges,[2] S.-J. Kim,[3] and D. J. Erickson[4]

Received 20 September 2011; revised 27 October 2011; accepted 27 October 2011; published 14 December 2011.

[1] Hourly winter weather of the Last Glacial Maximum (LGM) is simulated using the Community Climate Model version 3 (CCM3) on a globally resolved T170 (~75 km) grid. Results are compared to a longer LGM climatological run with the same boundary conditions and monthly saves. Hourly-scale animations are used to enhance interpretations. The purpose of the study is to explore whether additional insights into ice age conditions can be gleaned by going beyond the standard employment of monthly average model statistics to infer ice age weather and climate. Results for both LGM runs indicate a decrease in North Atlantic and increase in North Pacific cyclogenesis. Storm trajectories react to the mechanical forcing of the Laurentide Ice Sheet, with Pacific storms tracking over middle Alaska and northern Canada, terminating in the Labrador Sea. This result is coincident with other model results in also showing a significant reduction in Greenland wintertime precipitation – a response supported by ice core evidence. Higher-temporal resolution puts in sharper focus the close tracking of Pacific storms along the west coast of North America. This response is consistent with increased poleward heat transport in the LGM climatological run and could help explain "early" glacial warming inferred in this region from proxy climate records. Additional analyses shows a large increase in central Asian surface gustiness that support observational inferences that upper-level winds associated with Asian-Pacific storms transported Asian dust to Greenland during the LGM. **Citation:** Unterman, M. B., T. J. Crowley, K. I. Hodges, S.-J. Kim, and D. J. Erickson (2011), Paleometeorology: High resolution Northern Hemisphere wintertime mid-latitude dynamics during the Last Glacial Maximum, *Geophys. Res. Lett.*, *38*, L23702, doi:10.1029/2011GL049599.

1. Introduction

[2] Although high-resolution climate simulations play an increasing role in modeling present and future climates, application to past climates has been relatively infrequent. A high resolution regional model has been previously run for the Laurentide Ice Sheet sector [*Bromwich et al.*, 2004], but to the best of our knowledge this study encompasses the highest spatial and temporal resolution analysis on the global scale for the LGM [*Unterman*, 2007; *Kim et al.*, 2008]. The initial report on the LGM climatological run [*Kim et al.*, 2008] demonstrated that anomaly plots of temperature and precipitation could be more closely linked to geography than those at lower resolution. Furthermore, the size of the grid box (approx. 75 km) is more appropriate for validation against geological data on land (e.g., pollen, lakes), because those proxies are more representative of a domain about the same size as the model grid scale. Consequently, model-data comparison of glacial-interglacial land temperature differences yielded uncertainties one-half those obtained with the same model at T42 resolution.

[3] Herein, we examine hourly-scale winter circulation for the last glacial maximum (21,000 BP) – the most intensely studied climate interval in Earth history and one of the first targets for application of climate models to past climates [e.g., *Williams et al.*, 1974; *Gates*, 1976]. The purpose of this pilot study is to inquire into whether examination of higher-resolution simulations, on both spatial and temporal scales, can enhance meteorological/climatological inferences based on monthly-averaged statistics of model output. We focus on northern hemisphere winter winds, cyclogenesis, and storm tracks, and employ trajectory analysis and animations to aid interpretations. Such high spatially and temporally resolved climate models can more accurately portray storms and storm processes along the full length of a storm lifetime [e.g., *Blender and Schubert*, 2000; *Bengtsson et al.*, 2009]. The animations may also be of pedagogic value for introductory-level classes.

[4] We simulated one ice age winter at T170 spatial resolution and hourly temporal resolution, hereafter described as the "synoptic simulation". This amounts to approximately 1500 hours of simulation after discarding the first 500 hours as spin-up. From a climatological viewpoint, this short test might seem limited. From the meteorological perspective, the duration of our "record" is comparable to those obtained from large-scale field experiments such as GATE or TOGA-COARE, which have been of considerable value not only to the meteorological but also the climate communities [e.g., *Shin et al.*, 1990; *Webster and Lukas*, 1992]. Nevertheless, we recognize that a future longer-duration simulation at this resolution would be required to determine the representativeness of results presented here.

[5] An unexpected result of the synoptic run is that in some cases we found responses that could potentially be extrapolated to the longer glacial time scale. We employ this extrapolation only when results are consistent with our LGM climatological run, other models, and/or the geological data, always recognizing that "more work needs to be done"

[1]Grant Institute, School of Geosciences, University of Edinburgh, Edinburgh, UK.
[2]Environmental Systems Science Centre, University of Reading, Reading, UK.
[3]Korea Polar Research Institute, KORDI, Incheon, South Korea.
[4]Center for Computational Sciences, Oak Ridge National Laboratory, Oak Ridge, Tennessee, USA.

0094-8276/11/2011GL049599

before the conclusions can be accepted. Finally, we highlight a few observations that are intriguing targets for future detailed investigation.

2. Methods

[6] We have run the simulation using the same model and boundary conditions as discussed in more detail by *Kim et al.* [2008]. We will sometimes compare our results with the six-year Kim et al. study, which we refer to as the LGM climatological run. We use the Community Climate Model (CCM) version 3.6 (CCM 3.6.6 physics). Model resolution is roughly 75 km on a grid box side (T170). Although a total of 68 variables on 18 sigma levels were saved at hourly steps in the synoptic scale simulation, we primarily focus on winds, sea level pressure, temperature, and precipitation for this paper.

[7] Boundary conditions have atmospheric CO_2 reduced to 200 ppm. Sea level has been lowered 120 meters, and LGM ice sheet topography was taken from *Peltier*'s [1994] ICE-4G reconstruction. Although a more recent ice-sheet reconstruction is now available [*Peltier*, 2004], we kept the older ICE-4G reconstruction in the synoptic scale simulation for consistency between the two LGM simulations.

[8] Prescribed sea surface temperatures (SST) are derived from the work by *CLIMAP Project Members* [1981], except that temperatures have been uniformly lowered by 1°C to be more consistent with recent analyses [e.g., *Crowley*, 2000; *Ballantyne et al.*, 2005; cf. *MARGO Project Members*, 2009] and to maintain continuity with *Kim et al.*'s [2008] study. As a check on the 1°C adjustment, we compared simulated mean annual surface temperatures in the LGM climatological run over North America with noble gas groundwater temperatures (Figure S1 in the auxiliary material), which are generally considered the most reliable indicator of temperature changes on land.[1] Results indicate very good agreement, with the four groundwater sites differing by only 0.4°C with the climatological run using the modified CLIMAP SSTs (total difference for global borehole comparison is about 0.8°C [see *Kim et al.*, 2008, Table 2]).

[9] In the North Atlantic, winter sea ice limit was specified near 42°N. The original *McIntyre et al.* [1976] reconstruction and the recent *MARGO Project Members* [2009] reconstruction illustrate a northward indentation in the central North Atlantic. However, we kept the more zonal sea ice boundary in the synoptic run for the sake of consistency with *Kim et al.* [2008]. Our winter sea ice boundary can be considered an extreme limit, useful for testing the model response to this condition, but subject to future sensitivity testing. A cautionary flag must therefore be raised when assessing (especially) fine detail of North Atlantic storm tracks. We suspect however, that the indentation is not fundamental to explaining any of the principal results we obtain, as our general results for the North Atlantic sector are comparable to other studies [e.g., *Charles et al.*, 1994; *Langen and Vinther*, 2009; *Donohoe and Battisti*, 2009].

3. Results and Discussion

[10] We first compare the four year wintertime (DJF) sea level pressure (SLP) in the model modern climatological control run with the ERA40 re-analysis to determine if our climatological simulation is consistent with that represented by re-analysis data (Figure 1). The locations and intensities of the Aleutian and Icelandic lows and subtropical highs are comparable (see also Table S1). The eastward displacement of the Azores high is as expected for this version of the CCM [cf. *Hurrell et al.*, 1998].

[11] Although modern climatological control SLP in the Atlantic and Pacific lows are approximately equal, LGM Pacific-Atlantic differences are ~10 hPa in *Kim et al.*'s [2008] run. This result was also found by *Donohoe and Battisti* [2009]. Mean LGM sea level pressure in the North Pacific low for the Kim et al. run, adjusted for ~12 hPa glacial-interglacial offset due to sea level lowering [*Betts and Ridgway*, 1992], is only 3 hPa deeper than the modern climatological simulation, but the North Atlantic low in the LGM is ~8 hPa shallower. The weaker North Atlantic cyclogenesis is in part due to storms exiting the Pacific track too far north of the baroclinic zone in the North Atlantic [*Donohoe and Battisti*, 2009].

[12] The well-defined eastern North Atlantic low pressure core that is present in *Kim et al.*'s [2008] LGM run (cf. Figure 1) is absent in our synoptic simulation (or displaced far to the west). We suspect this discrepancy reflects an intraseasonal oscillation (not shown), resulting in an eastward diversion of Arctic outflow through the Siberian "Lena River Gap" (cf. Figure 2) between two Siberian ice sheets. Detailed features of the Atlantic sector of the synoptic run may therefore be less generalizable than for the Pacific case.

[13] Using the methodology of *Hoskins and Hodges* [2002], storm tracks reveal further information about mid-latitude flow (Figure 3). During the LGM the North Atlantic has 15.4% less intense storms (Figure S2) compared to the modern simulation. Even though this is a short run, the result is very comparable to the 17% of *Donohoe and Battisti* [2009]. In contrast, the North Pacific storms are 8% more intense. SLP trajectories show seven large-magnitude storms in the Pacific, with only one in the North Atlantic. Particularly notable is the tracking of storm systems along the west coast of North America, in the region where the climatological atmospheric polar heat transport is significantly greater than in the control simulation [*Kim et al.*, 2008, Figure 4].

[14] No storms track directly over Greenland; this result is further clarified in our high-resolution animations (cf. auxiliary material). Analysis of lysis points (not shown) in the synoptic scale simulation for Pacific sourced storms indicates some clustering in the Labrador Sea. In modern moisture source experiments [e.g., *Charles et al.*, 1994; *Langen and Vinther*, 2009], Greenland precipitation is derived from a wide range of source locations, including the North Atlantic and Greenland areas, North America, and the North Pacific. However, in the synoptic scale LGM simulation, there is a significant reduction in the wintertime Greenland precipitation rate ($\sim 1.6 \times 10^{-3}$ mm/hour) and total accumulation (3.5 mm), with ~25% of the total deposited over a week long event (the peak rate is $\sim 1.0 \times 10^{-2}$ mm/hour – at hours 628–894). The termini of storms west of Greenland, in the Labrador Sea, are derived from storms exiting the North Pacific track. The four LGM climatological winters in Kim et al. range from 2 mm to 6 mm total, as compared to 75 mm to 106 mm in the model control simulation (cf. Figure 2). Our results – both climatological

[1] Auxiliary materials are available in the HTML. doi:10.1029/2011GL049599.

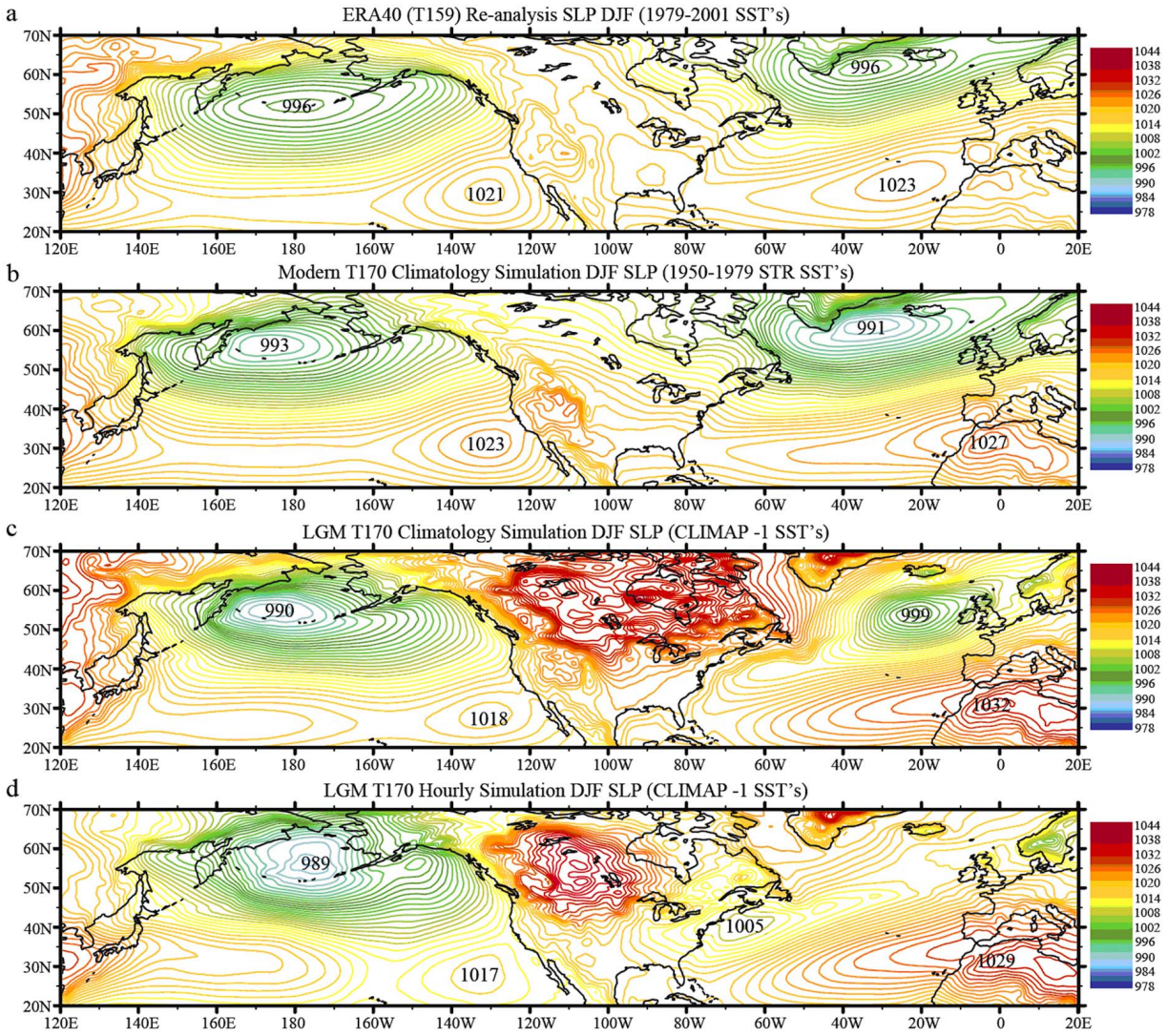

Figure 1. (a) ERA40 SLP data is compared to (b) the modern climatological simulation and (c, d) the two different simulations of the LGM. To aid in comparison with the present, LGM SLP has been decreased by 12 mb to account for the effect of 120 m in sea level lowering on surface pressure [*Betts and Ridgway*, 1992].

and synoptic - are consistent with observed decreased glacial accumulation rates in the Greenland ice cores [e.g., *Fawcett et al.*, 1997; *Johnsen et al.*, 2001].

[15] The synoptic-scale simulation portrays strong northerly flow along the full expanse of the extended North Atlantic sea ice field (Figures 2 and S3), feeding into the axis of the main storm track located a few degrees south of the sea ice margin [cf., e.g., *Manabe and Broccoli*, 1985; *Kageyama et al.*, 1999; *Kim et al.*, 2008]. The narrowness of this track in the high-resolution run could be a topic for further investigation, as it should be the site of intensified atmosphere–ocean interactions resulting in, for example, increased upwelling that could potentially be detectable in marine plankton data. Such focused air-sea interaction could also affect ice-age intermediate/deep water production [cf. *Häkkinen*, 1987; *Crowley and Häkkinen*, 1988].

[16] In the animations and the composite of hourly surface winds (Figure S4), it is also clear that Pacific cold air outbreaks extend equatorward in the west and central Pacific; intensified convection within the ITCZ is sometimes associated with these equatorial surges. The locations of the cold-air surges are consistent with the LGM climatological run showing decreased poleward heat transport in the western Pacific [*Kim et al.*, 2008, Figure 4] – a result that, if substantiated by other studies, could indicate a significant extratropical contributor to tropical cooling in the western Pacific sector.

[17] Average upper level winds indicate a slight "bowing" of the jet over North America (Figure 4), with a "modified" split jet [e.g., *Kutzbach and Wright*, 1985; *Manabe and Broccoli*, 1985; *Kim et al.*, 2008]. Synoptically however, there is a great deal of variability (Figure S5) as the jet fluctuates between several transient wave-forms. In two cases there is an extreme southward dip that subsequently "closes off", developing into a Kona Low [*Moore et al.*, 2008] in the subtropical Pacific (model hours 958 and 1152 of animation). The subtropical moisture source for these systems is very evident in the animation.

[18] Further analysis of surface and upper wind flow demonstrates that component wind velocities are not

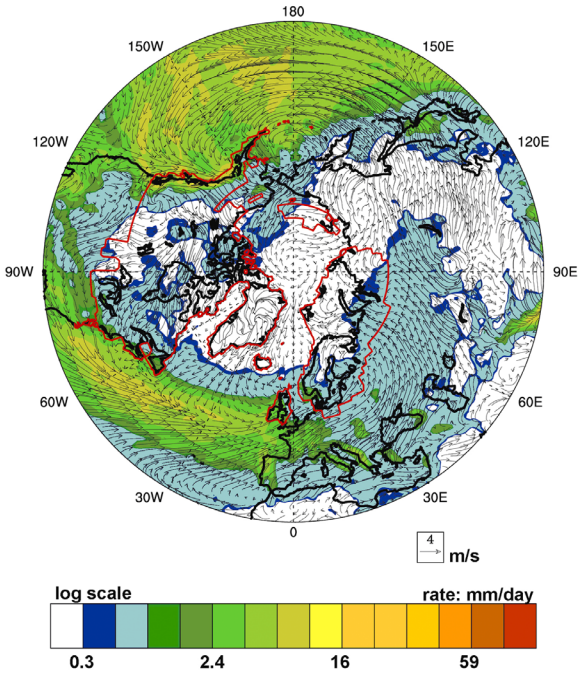

Figure 2. Synoptic scale simulation of mean total precipitation and surface wind flow during wintertime LGM. Red outlines denote ice sheet margins.

necessarily normally distributed around the mean. Although the mean upper air velocity is near zero over central Greenland (Figure 4b), the distribution in this region is not normal, showing a distinct secondary mode of higher velocities from the west that can be linked to some of the extreme Pacific storms in Figure 3 (e.g., two large Pacific storms at hours 737–822, and 816–901).

[19] This result is of interest because the LGM Greenland dust source was probably from Asia [*Biscaye et al.*, 1997], and upper air transport changes in the extreme events, not clearly evident in the seasonal average, may have provided conditions responsible for the deposition. In examining this issue more closely, we find a two fold increase in the percentage of surface wind events over the 16 m/s and 8 m/s thresholds for the Central Loess Plateau in Asia, and a three fold increase for the thresholds in the Taklamakan Desert. The increase in hourly wind intensities over dust source locations during the LGM should further contribute to the greater dust source emissions seen in ice cores. The results in the synoptic run are consistent with large surface stress values in the LGM climatological run in this region (not shown). With such gust events, the top 0.1% of synoptic scale wind events may account for over 50% of the total atmospheric dust burden [cf. *McGee et al.*, 2010].

4. Summary and Conclusions

[20] Our results are consistent with other model simulations showing significant reductions in Atlantic cyclogenesis, stronger Pacific cyclogenesis, and low wintertime accumulation on Greenland during the LGM. The novel contribution of this study is the use of high temporal resolution of model output in order to clearly resolve weather systems in the ice age. Specific results that are new, or appear more clearly in high-resolution runs, involve tracking of Pacific lows up the west coast of North America, sharpness of the Atlantic storm trajectory along the edge of the expanded sea ice margin, extension of Asian-Pacific high pressure outbreaks to the equator, and rare events in the upper air flow pattern over Greenland that can be linked to strong Pacific storms triggered by Asian cold-air outbreaks in the area of origin of ice-age dust. These regions are also impacted by hourly wind events over the 16 m/s and 8 m/s thresholds. These latter results may explain conditions favorable for deposition of Asian dust in Greenland ice cores during this time [*Biscaye et al.*, 1997].

[21] While our results require more testing, the consistency of some results with either the climatological run, other models, and/or geological data suggest that, at least in some cases, high-resolution runs can provide valuable insight to add to the cornucopia of information already available from lower-resolution runs. In particular, this one-season tracking of Pacific storms up the west coast of North America is apparently representative of mean annual climatological conditions, as it is consistent with increased

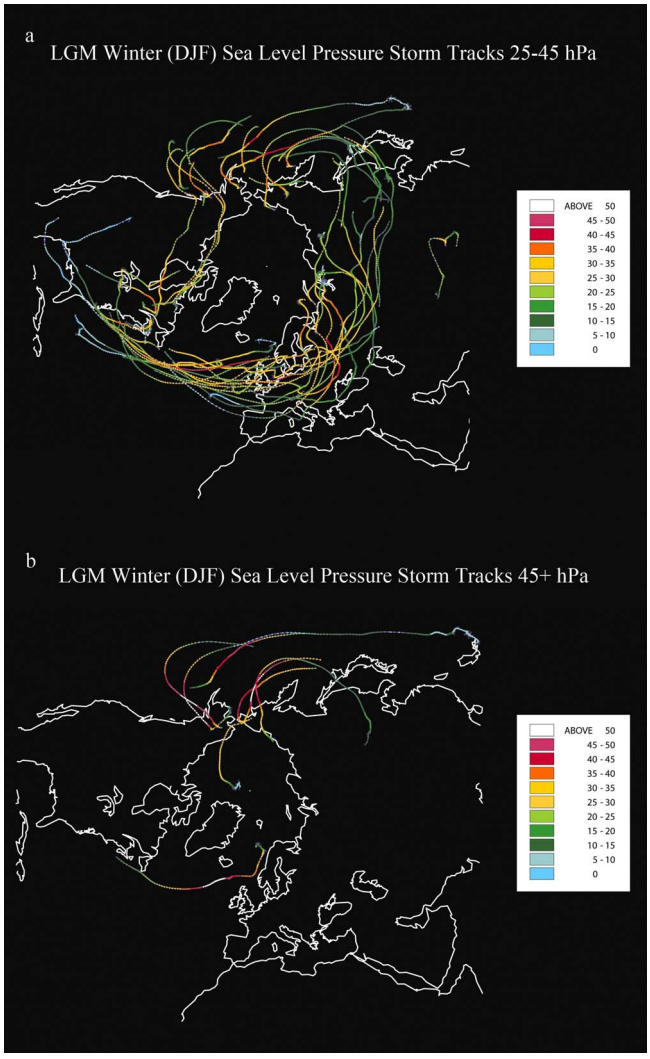

Figure 3. LGM storm trajectories using sea level pressure [cf. *Hoskins and Hodges*, 2002]. Note the narrow North Atlantic storm tack over the sea ice margin and the northerly diversion of large Pacific storms over middle Alaska.

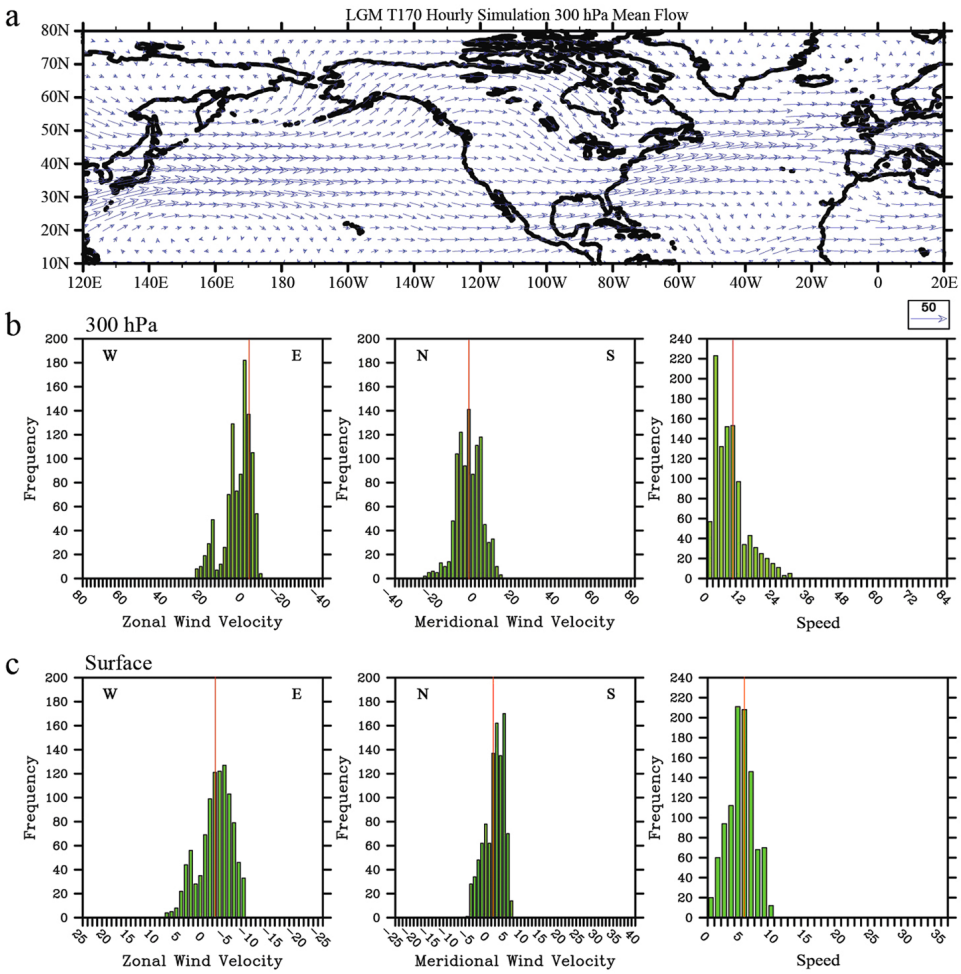

Figure 4. (a) Mean 300 hPa wind flow in the synoptic scale animation, (b) frequency of component wind velocities at 300 hPa and (c) the surface for 72°N, 38°W. Red line denotes mean velocity. Wind direction is listed as N, S, E and W where N denotes northerly wind.

atmospheric heat transport in the LGM climatological run. It is also consistent with glacial-maximum warming in coastal and nearby land areas [*Winograd et al.*, 1992; *Ludwig et al.*, 1992; *Herbert et al.*, 2001], rising levels of Great Basin Lakes [*Benson et al.*, 1990], and glacial *advance* farther north [e.g., *Young et al.*, 2011]. In a future study, we plan to investigate the consistency between modelled and observed changes in this region.

[22] **Acknowledgments.** We thank the Center for Computational Science (CCS) team at ORNL for making this work possible and the British Atmospheric Data Centre (BADC) for access to ERA40 data sets. This study was supported by ORNL and the University Of Edinburgh School of Geosciences, in conjunction with the Scottish Alliance for Geosciences, Environment and Society (SAGES). Seong-Joong Kim was supported by the project "Paleoclimate Modelling Study for Polar Regions (PE08140)" of the Korea Polar Research Institute.

[23] The Editor thanks the two anonymous reviewers for their assistance in evaluating this paper.

References

Ballantyne, A. P., M. Lavine, T. J. Crowley, J. Liu, and P. B. Baker (2005), Meta-analysis of tropical surface temperatures during the Last Glacial Maximum, *Geophys. Res. Lett.*, *32*, L05712, doi:10.1029/2004GL021217.

Bengtsson, L., K. I. Hodges, and N. Keenlyside (2009), Will extra-tropical storms intensify in a warmer climate?, *J. Clim.*, *22*, 2276–2301, doi:10.1175/2008JCLI2678.1.

Benson, L. V., et al. (1990), Chronology of expansion and contraction of 4 Great Basin lake systems during the past 35,000 years, *Palaeogeogr. Palaeoclimatol. Palaeoecol.*, *78*, 241–286, doi:10.1016/0031-0182(90)90217-U.

Betts, A. K., and W. Ridgway (1992), Tropical boundary layer equilibrium in the last ice age, *J. Geophys. Res.*, *97*, 2529–2534, doi:10.1029/91JD02974.

Biscaye, P. E., F. E. Grousset, M. Revel, S. Van der Gaast, G. A. Zielinski, A. Vaars, and G. Kukla (1997), Asian provenance of glacial dust (stage 2) in the Greenland Ice Sheet Project 2 Ice Core, Summit, Greenland, *J. Geophys. Res.*, *102*, 26,765–26,781, doi:10.1029/97JC01249.

Blender, R., and M. Schubert (2000), Cyclone tracking in different spatial and temporal resolutions, *Mon. Weath. Rev.*, *128*, 377–383.

Bromwich, D. H., et al. (2004), Polar MM5 simulations of the winter climate of the Laurentide Ice Sheet at the LGM, *J. Clim.*, *17*, 3415–3433, doi:10.1175/1520-0442(2004)017<3415:PMSOTW>2.0.CO;2.

Charles, C. D., et al. (1994), Glacial-interglacial changes in moisture sources for Greenland: Influences on the ice core record of climate, *Science*, *263*, 508–511, doi:10.1126/science.263.5146.508.

CLIMAP Project Members (1981), Seasonal reconstructions of the Earth's surface at the Last Glacial Maximum, Map Chart Ser. MC36, Geol. Soc. Am., Boulder, Colo.

Crowley, T. J. (2000), CLIMAP SSTs re-revisited, *Clim. Dyn.*, *16*, 241–255, doi:10.1007/s003820050325.

Crowley, T. J., and S. Häkkinen (1988), A new mechanism for decreasing North Atlantic Deep Water production rates in the Pleistocene, *Paleoceanography*, *3*, 249–258, doi:10.1029/PA003i003p00249.

Donohoe, A., and D. S. Battisti (2009), Causes of reduced North Atlantic storm activity in a CAM3 simulation of the Last Glacial Maximum, *J. Clim.*, *22*, 4793–4808, doi:10.1175/2009JCLI2776.1.

Fawcett, P. J., A. M. Ágústsdóttir, R. B. Alley, and C. A. Shuman (1997), The Younger Dryas termination and North Atlantic Deep Water formation: Insights from climate model simulations and Greenland ice cores, *Paleoceanography*, *12*, 23–38, doi:10.1029/96PA02711.

Gates, W. L. (1976), The numerical simulation of ice-age climate with a global general circulation model, *J. Atmos. Sci.*, *33*, 1844–1873, doi:10.1175/1520-0469(1976)033<1844:TNSOIA>2.0.CO;2.

Häkkinen, S. (1987), A coupled dynamic-thermodynamic model of an ice-ocean system in the marginal ice zone, *J. Geophys. Res.*, *92*, 9469–9478, doi:10.1029/JC092iC09p09469.

Herbert, T. D., et al. (2001), Collapse of the California Current during glacial maxima linked to climate change on land, *Science*, *293*, 71–76, doi:10.1126/science.1059209.

Hoskins, B. J., and K. I. Hodges (2002), New perspectives on the Northern Hemisphere winter storm tracks, *J. Atmos. Sci.*, *59*, 1041–1061, doi:10.1175/1520-0469(2002)059<1041:NPOTNH>2.0.CO;2.

Hurrell, J. W., et al. (1998), The dynamical simulation of the NCAR Community Climate Model version 3 (CCM3), *J. Clim.*, *11*, 1207–1236, doi:10.1175/1520-0442(1998)011<1207:TDSOTN>2.0.CO;2.

Johnsen, S. J., et al. (2001), Oxygen isotope and palaeotemperature records from six Greenland ice-core stations: Camp Century, Dye-3, GRIP, GISP2, Renland and NorthGRIP, *J. Quat. Sci.*, *16*, 299–307, doi:10.1002/jqs.622.

Kageyama, M., et al. (1999), Northern hemisphere storm tracks in present day and Last Glacial Maximum climate simulations: A comparison of the European PMIP models, *J. Clim.*, *12*, 742–760, doi:10.1175/1520-0442(1999)012<0742:NHSTIP>2.0.CO;2.

Kim, S., et al. (2008), High-resolution climate simulation of the Last Glacial Maximum, *Clim. Dyn.*, *31*, 1–16, doi:10.1007/s00382-007-0332-z.

Kutzbach, J. E., and H. E. Wright Jr. (1985), Simulation of the climate of 18,000 yr BP: Results for the North American/North Atlantic/European sector, *Quat. Sci. Rev.*, *4*, 147–187, doi:10.1016/0277-3791(85)90024-1.

Langen, P. L., and B. M. Vinther (2009), Response in atmospheric circulation and sources of Greenland precipitation to glacial boundary conditions, *Clim. Dyn.*, *32*, 1035–1054, doi:10.1007/s00382-008-0438-y.

Ludwig, K. R., et al. (1992), Mass-Spectrometric ^{230}Th-^{234}U-^{238}U dating of the Devils Hole calcite vein, *Science*, *258*, 284–287, doi:10.1126/science.258.5080.284.

Manabe, S., and A. J. Broccoli (1985), The influence of continental ice sheets on the climate of an ice age, *J. Geophys. Res.*, *90*, 2167–2190, doi:10.1029/JD090iD01p02167.

MARGO Project Members (2009), Constraints on the magnitude and patterns of ocean cooling at the Last Glacial Maximum, *Nat. Geosci.*, *2*, 127–132, doi:10.1038/ngeo411.

McGee, D., W. S. Broecker, and G. Winckler (2010), Gustiness: The driver of glacial dustiness?, *Quat. Sci. Rev.*, *29*, 2340–2350, doi:10.1016/j.quascirev.2010.06.009.

McIntyre, A., et al. (1976), Glacial North Atlantic 18,000 years ago: A CLIMAP reconstruction, *Mem. Geol. Soc. Am.*, *145*, 43–76.

Moore, R. W., O. Martius, and H. C. Davies (2008), Downstream development and Kona Low genesis, *Geophys. Res. Lett.*, *35*, L20814, doi:10.1029/2008GL035502.

Peltier, W. R. (1994), Ice Age paleotopography, *Science*, *265*, 195–201, doi:10.1126/science.265.5169.195.

Peltier, W. R. (2004), Global glacial isostasy and the surface of the ice-age earth: The ICE-5G (Vm2) model and GRACE, *Annu. Rev. Earth Planet. Sci.*, *32*, 111–149, doi:10.1146/annurev.earth.32.082503.144359.

Shin, K.-S., et al. (1990), Time scales and variability of area-averaged tropical oceanic rainfall, *Mon. Weather Rev.*, *118*, 1507–1516, doi:10.1175/1520-0493(1990)118<1507:TSAVOA>2.0.CO;2.

Unterman, M. B. (2007), High resolution simulations of synoptic scale meteorology for the Last Glacial Maximum, M.S. thesis, Duke Univ., Durham, N. C.

Webster, P. J., and R. Lukas (1992), TOGA COARE: The Coupled Ocean–atmosphere Response Experiment, *Bull. Am. Meteorol. Soc.*, *73*, 1377–1416, doi:10.1175/1520-0477(1992)073<1377:TCTCOR>2.0.CO;2.

Williams, J., R. G. Barry, and W. M. Washington (1974), Simulation of the atmospheric circulation using the NCAR global circulation model with ice age boundary conditions, *J. Appl. Meteorol.*, *13*, 305–317, doi:10.1175/1520-0450(1974)013<0305:SOTACU>2.0.CO;2.

Winograd, I. J., et al. (1992), Continuous 500,000-year climate record from vein calcite in Devils Hole, Nevada, *Science*, *258*, 255–260, doi:10.1126/science.258.5080.255.

Young, N. E., et al. (2011), Assessing climatic and nonclimatic forcing of Pinedale glaciation and deglaciation in the western United States, *Geology*, *39*, 171–174, doi:10.1130/G31527.1.

T. J. Crowley and M. B. Unterman, Grant Institute, School of Geosciences, University of Edinburgh, West Mains Road, Edinburgh EH9 3JW, UK. (m.b.unterman@sms.ed.ac.uk)

D. J. Erickson, Center for Computational Sciences, Oak Ridge National Laboratory, PO Box 2008, Oak Ridge, TN 37831, USA.

K. I. Hodges, Environmental Systems Science Centre, University of Reading, Harry Pitt Building, 3 Earley Gate, Reading RG6 6AL, UK.

S.-J. Kim, Korea Polar Research Institute, KORDI, Incheon 406-840, South Korea.